

## STUDIES OF TWO-BODY $\beta$ -DECAYS AT THE FRS-ESR FACILITY\*

J. KURCEWICZ<sup>a</sup>, F. BOSCH<sup>a</sup>, H. GEISSEL<sup>a,b</sup>, YU.A. LITVINOV<sup>a,c</sup>  
 N. WINCKLER<sup>a,c</sup>, K. BECKERT<sup>a</sup>, P. BELLER<sup>a†</sup> D. BOUTIN<sup>a,d</sup>  
 C. BRANDAU<sup>a</sup>, L. CHEN<sup>b</sup>, C. DIMOPOULOU<sup>a</sup>, H.G. ESSEL<sup>a</sup>, B. FABIAN<sup>b</sup>  
 T. FAESTERMANN<sup>e</sup>, A. FRAGNER<sup>f</sup>, B. FRANZKE<sup>a</sup>, E. HAETTNER<sup>b</sup>  
 M. HAUSMANN<sup>g</sup>, S. HESS<sup>a</sup>, P. KIENLE<sup>e,f</sup>, R. KNÖBEL<sup>a,b</sup>  
 C. KOZHUHAROV<sup>a</sup>, S.A. LITVINOV<sup>a</sup>, L. MAIER<sup>e</sup>, M. MAZZOCCO<sup>a,h</sup>  
 F. MONTES<sup>a,g</sup>, A. MUSUMARRA<sup>i,j</sup>, C. NOCIFORO<sup>a</sup>, F. NOLDEN<sup>a</sup>  
 Z. PATYK<sup>k</sup>, W.R. PLASS<sup>a</sup>, A. PROCHAZKA<sup>a</sup>, R. REDA<sup>f</sup>, R. REUSCHL<sup>a</sup>  
 C. SCHEIDENBERGER<sup>a,b</sup>, M. STECK<sup>a</sup>, T. STÖHLKER<sup>a,l</sup>, B. SUN<sup>a,m</sup>  
 K. TAKAHASHI<sup>n</sup>, S. TORILOV<sup>o</sup>, M. TRASSINELLI<sup>a</sup>, H. WEICK<sup>a</sup>  
 M. WINKLER<sup>a</sup>

<sup>a</sup>GSI Helmholtzzentrum für Schwerionenforschung, Darmstadt, Germany

<sup>b</sup>Justus-Liebig-Universität, Gießen, Germany

<sup>c</sup>Max-Planck-Institut für Kernphysik, Heidelberg, Germany

<sup>d</sup>Service de Physique Nucléaire CEA, Saclay, France

<sup>e</sup>Technische Universität München, München, Germany

<sup>f</sup>Stefan-Meyer-Institut für subatomare Physik, Vienna, Austria

<sup>g</sup>Michigan State University, East Lansing, USA

<sup>h</sup>INFN Padova, Italy

<sup>i</sup>Laboratori Nazionali del Sud, INFN Catania, Italy

<sup>j</sup>University of Catania, Italy

<sup>k</sup>A. Sołtan Institute for Nuclear Studies, Warsaw, Poland

<sup>l</sup>Ruprecht-Karls Universität, Heidelberg, Germany

<sup>m</sup>Beihang University, Beijing 100191, China

<sup>n</sup>Université Libre de Bruxelles, Bruxelles, Belgium

<sup>o</sup>St. Petersburg University, Russia

*(Received December 15, 2009)*

A combination of the in-flight projectile fragment separator and the heavy-ion storage-cooler ring has been used to produce, store and investigate cooled highly charged ions. The results of recently performed experiments at GSI Darmstadt studying two-body  $\beta$ -decays of H-like and He-like ions are presented. The technique of Schottky lifetime spectroscopy has been applied to explore the electron capture and bound-state  $\beta^-$  decay processes of ions circulating in the heavy-ion storage ring.

PACS numbers: 21.10.Tg, 23.40.-s, 31.30.Gs, 23.40.Bw

---

\* Presented at the XXXI Mazurian Lakes Conference on Physics, Piaski, Poland, August 30–September 6, 2009.

† Deceased.

## 1. Introduction

In the last two decades storage rings have proved to be a very powerful and versatile tool for studying nuclear and atomic properties of highly charged heavy ions. It became possible to carry out  $\beta$ -decay studies of nuclear systems in conditions similar to those in stellar environments where the mean atomic charge state remains high as well. This has a large impact on deeper understanding of the nucleosynthesis process.

It has been recognized very soon that the number of electrons bound in the atom could modify considerably the lifetime of the corresponding nucleus [1].  $^{163}\text{Dy}$  is stable as a neutral atom, however, as a fully stripped can decay by emission of the decay electron into the  $K$  and  $L$  shells of the daughter atom [2]. Neutral  $^{187}\text{Re}$  is known for its notably long half-life of 43 Gy, however, bare  $^{187}\text{Re}$  is unstable against bound-state  $\beta^-$  decay with the electron bound in the  $K$ -shell and decays by nine orders of magnitude faster.

Neither the electron capture decay mode nor the internal conversion of isomeric transitions can proceed after removal of all shell electrons. By using fully ionized fragments it is possible to study the  $\beta^+$ -decay alone as it was done in an experiment investigating bare  $^{52}\text{Fe}^{26+}$  ions [3].

Storage rings are moreover an irreplaceable tool for performing precise mass measurements. The complementary methods of mass measurements namely the Schottky Mass Spectrometry and Isochronous Mass Spectrometry allow us to approach nuclides with extremely different life times. Both methods were developed at the ESR of GSI [4].

The  $\beta$  lifetimes together with the masses are the basic ingredients for re-drawing the pathways of stellar nucleosynthesis in the s-, rp- and r-processes. Precise lifetimes and mass measurements are of great importance for exploring the limits of nuclear stability.

## 2. Experimental method

The experimental facilities at GSI/Darmstadt offer unique opportunity for the production, storage and cooling of radioactive beams. All stable isotopes from hydrogen up to uranium can be accelerated by the linear accelerator UNILAC and the SIS synchrotron up to energies around 1 GeV/ $u$ . After leaving the synchrotron the primary beam impinges on a target (around 1–4 g/cm<sup>2</sup> thick) located at the entrance to the Fragment Separator (FRS). From the vast mixture of projectile fragments highly-charged nuclides of interest are selected by means of the  $B\rho-\Delta E-B\rho$  method [5] and injected into the Experimental Storage Ring (ESR) [6]. The ESR consisting of two arcs and two straight sections has a circumference of about 108 m and is capable of storing ions with magnetic rigidity between 0.5 and 10 Tm. The beamline of the ESR is equipped with a set of Schottky noise probes which collect the

mirror charge of each passing ion, thus providing the information about its revolution frequency. In case of two different ions their revolution frequencies  $f_i$  and  $f_j$  can be related to their relative difference of the  $(m/q)$ -ratios by the following expression:

$$\frac{f_j - f_i}{f_i} = -\frac{1}{\gamma_t^2} \frac{(m/q)_j - (m/q)_i}{(m/q)_i} + \frac{v_j - v_i}{v_i} \left(1 - \frac{\gamma^2}{\gamma_t^2}\right), \quad (1)$$

where  $v_j, v_i$  are the ions velocities,  $\gamma$  is the Lorentz factor,  $\gamma_t = 1/\sqrt{\alpha_p}$  and  $\alpha_p$  is the momentum compaction factor characterizing the relative variation of the orbital length per relative variation of the magnetic rigidity [7]. In the experiments described in this contribution both, stochastic [8, 9] and electron [10, 11] cooling were applied in order to decrease the velocity spread of the circulating ions, thus making the second term in Eq. (1) negligible. Then a one-to-one correspondence between the relative revolution frequencies and the relative  $(m/q)$ -ratio could have been established, yielding a high mass resolving power and providing an unambiguous isotopic and charge state identification. This approach is the basis of the Schottky Mass Spectrometry method [7, 12, 13].

The longitudinal momentum spread  $dp/p$  is determined by an equilibrium of cooling forces from the applied cooling technique and counteracting heating effects, such as intra-beam scattering. With electron cooling, momentum spreads  $dp/p$  in the order of  $10^{-6}$  and below are routinely achieved at the ESR for low intensity ion beams [12].

The ions stored in the ESR were circulating with revolution frequencies of about 2 MHz. The high harmonic (30–31st) of the noise signal generated in the Schottky pick-up electrodes was amplified and mixed down with a local oscillator providing a reference frequency. The difference signal in the frequency range of 0–300 kHz was digitized by using a 16-bit ADC and a Fast Fourier Transformation was applied to the data yielding revolution frequency spectra of the coasting ions.

The integrated noise power in each harmonic of the Schottky spectrum (peak area) is a constant and proportional to  $Nq^2f_0^2$ , where  $N$  is the total number of the stored ions,  $q$  is their charge state and  $f_0$  the mean revolution frequency. Thus, Schottky spectroscopy allows particle counting by the measurement of area in frequency peaks and nuclear lifetimes can be obtained from the measured time evolution of these peak areas [12].

### 3. Two-body $\beta$ -decay studies

The FRS-ESR facility combined with its detection setup is a perfect tool for performing  $\beta$ -decay studies of highly charged nuclides, providing a unique opportunity of selecting a particular decay branch [14]. In this contribution we will focus mainly on the two-body  $\beta$ -decay modes *i.e.* the

orbital electron capture and the bound-state  $\beta^-$  decay. A notable fact is that in two-body  $\beta$ -decays the atomic charge of the decaying nuclide does not change. Thus, the revolution frequency of the daughter ions remains very similar to the revolution frequency of the parent ions and the small difference between frequency peaks directly corresponds to the difference in mass (see Eq. (1)).

### 3.1. Orbital electron capture

Recently for the first time the measurements of the  $\beta^+$  and orbital electron-capture decay rates of bare, H-like and He-like  $^{140}\text{Pr}$  have been performed at GSI [15, 16]. The  $^{140}\text{Pr}$  nuclei have been produced via projectile fragmentation of a 508 MeV/ $u$   $^{152}\text{Sm}$  beam on a 1 g/cm<sup>2</sup> thick beryllium target. The beam intensity was of the order of  $3 \times 10^9$  ions/spill and the charge states of interest of  $^{140}\text{Pr}$  were separated by the in-flight fragment separator FRS (see Sec. 2).

Analyzing the frequency peaks present in the subsequently accumulated Schottky spectra, a time distribution of the number of H-like Pr and the  $\beta$ -decay daughter Ce ions stored in the ESR was constructed. In general, the time evolution of the number of mother activity ions can be described by the following expression

$$N_M(t) = N_M(0) e^{-\lambda t}, \quad (2)$$

where  $N_M(0)$  is the number of stored mother ions at the beginning of the measurement and  $\lambda = \lambda_{\beta^+} + \lambda_{\text{EC}} + \lambda_{\text{loss}}$  is the decay constant consisting of three components responsible for  $\beta^+$ -decay, electron capture decay and non-radioactive losses in the ring, respectively. In the case of the daughter activity the number of stored ions is given by

$$N_D(t) = N_M(0) \frac{\lambda_{\text{EC}}}{\lambda - \lambda_{\text{loss}}} \left( e^{-\lambda_{\text{loss}} t} - e^{-\lambda t} \right) + N_D(0) e^{-\lambda_{\text{loss}} t}, \quad (3)$$

where  $N_D(0)$  is the number of the daughter ions at the beginning of the measurement. We stress that events present in the frequency peak of the daughter ion originate only from the electron capture transition. The products of the continuum  $\beta^+$ -decay have a different ( $m/q$ )-ratio, therefore events corresponding to that decay branch are being placed in a distant range of the revolution frequency spectrum.

The H-like  $^{140}\text{Pr}^{58+}$  decay rate was found to be larger by a factor of 1.5 than in the case of He-like  $^{140}\text{Pr}^{57+}$  ion. This appears to be in contrast to the simple approximation suggesting that the orbital capture probability is proportional to the number of orbital  $K$  electrons. In particular, the decay

rate for H-like ions  $\lambda_{\text{H}}$  should be related to the decay rate of a He-like ions by the following expression [17]

$$\lambda_{\text{H}} = \frac{1}{2} \lambda_{\text{He}}. \quad (4)$$

However, the experimental result  $\lambda_{\text{H}} = 1.49(8)\lambda_{\text{He}}$  exceeds the simple prediction almost by a factor of three. This non-intuitive result can be explained by taking into account hyperfine splitting of nuclear levels in the decaying nuclei and the conservation law of the total angular momentum. In the case of H-like  $^{140}\text{Pr}$  atoms the hyperfine interaction between the electron and the nucleus splits the  $I_i = 1$  nuclear state into two levels with a total angular momentum of  $F = 1/2$  and  $F = 3/2$ . In the final state the total angular momentum of the system can only have one value  $F = 1/2$ , deriving from the coupling of the  $I_f = 0$  angular momentum of the  $^{140}\text{Ce}$  nucleus and the  $s = 1/2$  spin of the emitted neutrino. Based on the systematics of neighboring odd- $A$  nuclei the value of the magnetic moment of  $^{140}\text{Pr}$  was deduced to be  $\mu = +2.5\mu_N$  [18], hence, the lower hyperfine state is assigned to the  $F = 1/2$  level. Therefore, only transitions from the  $F = 1/2$  hyperfine level can participate in the allowed decay to the final state in  $^{140}\text{Ce}$ .

Indeed a detailed derivation shows [19] that for the  $\Delta I = I_f - I_i = -1$  electron capture transitions

$$\lambda_{\text{H}} = \frac{3}{2} \lambda_{\text{He}}, \quad (5)$$

which is in very good agreement with the experimental value. Recent calculations taking into account the electron screening of the electric charge of the nucleus in the He-like  $^{140}\text{Pr}^{57+}$  ion provides a decay constant ratio of  $\lambda_{\text{H}}/\lambda_{\text{He}} = 1.50(4)$  which agrees with the experimental result very well [20]. This findings have been confirmed in a recent experiment performed at GSI where the decay rates of both H-like and He-like  $^{142}\text{Pm}$  have been measured [21]. The  $^{142}\text{Pm}$  nuclei decay by 96.4% via allowed Gamow-Teller transition ( $1^+ \rightarrow 0^+$ ) to the stable ground state of the  $^{142}\text{Nd}^{60+}$  daughter nuclei. The ratio of the electron capture decay constants of H-like and He-like ions was found to be  $\lambda_{\text{H}} = 1.44(6)\lambda_{\text{He}}$  which is consistent with the theoretical predictions.

### 3.2. Bound-state $\beta^-$ decay

Bound-state  $\beta^-$ -decay ( $\beta_b$ ), the time-mirrored orbital electron capture process, was experimentally discovered [2] and further explored in experiments involving the ESR [22,25]. In this contribution we report on the direct observation of bound-state  $\beta^-$ -decays of fully-ionized  $^{205}\text{Hg}^{80+}$  and  $^{207}\text{Tl}^{81+}$  atoms.

The experiment was performed at the SIS synchrotron of GSI Darmstadt, which delivered a 750 A GeV  $^{208}\text{Pb}$  beam with an intensity of the order of  $10^9$  ions/spill. The ions of interest  $^{205}\text{Hg}$  and  $^{207}\text{Tl}$  were produced in the projectile fragmentation reaction. The 4 g/cm<sup>2</sup> thick beryllium target was placed at the entrance to the FRS. After passing the magnetic sections of the separator the selected ions were injected into the ESR, where they could remain for extended periods of time circulating with an energy of 400 MeV/ $u$  which corresponds to a revolution frequency of the order of 2 MHz.

The result of a typical measurement taken during a 2000 s run is shown in Fig. 1. The subsequently acquired Schottky noise FFT frames form a 2 D histogram showing the time evolution of the given range of the frequency spectrum. The peak intensity corresponds to the number of stored  $^{205}\text{Hg}^{80+}$  and  $^{205}\text{Tl}^{80+}$  ions (left panel). The frequency gap between the traces corresponding to mother and daughter ions is directly related to the mass difference of these species (see Eq. (1)). The fluctuations in the revolution frequencies are due to random instabilities of magnetic field and power supplies for the electron cooler. The presented spectra are the result of averaging over 10.5 s (100 FFT frames).

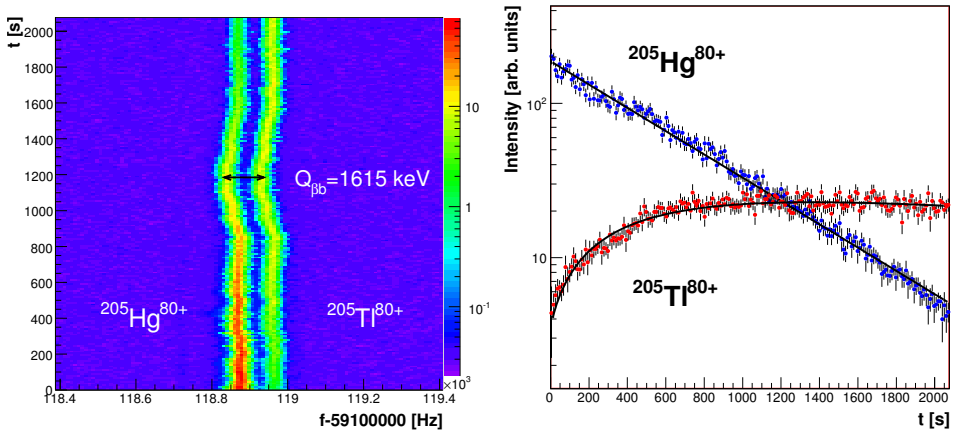


Fig. 1. Left panel: time evolution of the Schottky noise power density measured in the laboratory frame. The intensity of the traces corresponds to the number of stored  $^{205}\text{Hg}^{80+}$  and  $^{205}\text{Tl}^{80+}$  ions. The fluctuations in the revolution frequencies are due to random instabilities of magnetic field and power supplies for the electron cooler. The presented spectra are the result of averaging over 10.5 s (100 FFT frames). Right panel: time distribution of the peak intensity corresponding to number of stored  $^{205}\text{Hg}^{80+}$  and  $^{205}\text{Tl}^{80+}$  ions. The continuous line shows the fitted theoretical dependence given by Eqs. (2) and (3). Data were taken during one single measurement.

Analyzing the area of frequency peaks present in the subsequently accumulated Schottky spectra, for each pair of investigated nuclei a time distribution of the number of mother and daughter ions stored in the ESR was constructed (see the right panel in Fig. 1). The obtained time distributions were fitted with functions given by Eqs. (2) and (3), changing only the total decay rate to  $\lambda = \lambda_{\beta_b} + \lambda_{\beta_c} + \lambda_{\text{loss}}$  and replacing the electron capture decay rate  $\lambda_{\text{EC}}$  by the bound-state  $\beta^-$  decay rate. The fitted decay rate values are given in Table I. The obtained results are in good overall agreement with the predictions of the theory employing spectra of allowed transition [23], however, particularly for  $^{205}\text{Hg}$  showing the value of the  $\lambda_{\beta_c}$  almost 25% lower comparing with the calculations. This is confirmed by a recent theoretical work which provides for bare  $^{205}\text{Hg}^{80+}$  the continuous  $\beta^-$ -decay rate value of  $\lambda_{\beta_c} = 2.34 \times 10^{-3}$  s [24]. The only possible comparison with available experimental data, namely the  $\lambda_{\beta_b}$  and  $\lambda_{\beta_c}$  values for  $^{207}\text{Tl}$  [25] shows consistency with the result of the the experiment described in this work.

TABLE I

Decay rates  $\lambda_{\beta_b}$ ,  $\lambda_{\beta_c}$ , the  $Q_{\beta_b}$  value and the theoretical decay rates  $\lambda_{\beta_b}^{\text{th}}$ ,  $\lambda_{\beta_c}^{\text{th}}$  for fully stripped  $^{205}\text{Hg}$  and  $^{207}\text{Tl}$  ions obtained in this work and compared with the results from Ref. [25]. All decay rates are given in the ions eigenframe.

Ion	$\lambda_{\beta_b}$	$\lambda_{\beta_b}^{\text{th}}$	$\lambda_{\beta_c}$ $\times 10^{-4}$ [s $^{-1}$ ]	$\lambda_{\beta_c}^{\text{th}}$	$\lambda_{\beta_c}^{\text{neut}}$	$Q_{\beta_b}$ [keV]
$^{205}\text{Hg}^{80+}$	3.7(3)	3.21	16.9(14)	22.1	22.5(4)	1615(3)
$^{207}\text{Tl}^{81+}$	4.2(4)	4.06	20.3(9)	23.7	24.2(1)	1511(6)
	4.29(29) <sup>a</sup>		22.9(12) <sup>a</sup>			

<sup>a</sup> From Ref. [25].

### 3.3. Single particle decay spectroscopy

As it has been shown in previous studies the Schottky noise spectroscopy might extend its detection limit to single stored ion for nuclear charges  $Z > 30$  [26, 27]. Based on this unique feature a set of experiments was proposed focused on investigation of the electron capture phenomenon in H-like heavy ions. Shortly later the first measurement of the H-like  $^{140}\text{Pr}^{58+}$  was performed. This research program was successfully continued and other H-like systems like  $^{142}\text{Pm}^{60+}$  and  $^{122}\text{I}^{52+}$  were investigated as well.

The experiments were carried out in a particular mode restricting the number of ions injected into the ESR. In such case a clear correlation between the decrease of the intensity of the trace in the Schottky noise spectrum corresponding to the mother ions and the intensity increase of the daughter ions trace could be visible (see Fig. 2).

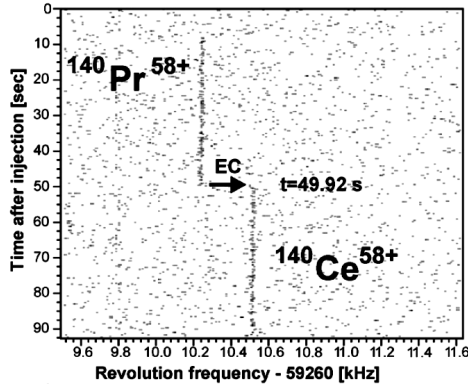


Fig. 2. Schottky noise power density spectra consecutively measured for  $^{140}\text{Pr}^{58+}$  in the laboratory frame. The single  $^{140}\text{Pr}^{58+}$  ion decaying to the daughter  $^{140}\text{Ce}^{58+}$  49.92 s after the injection into the ESR [28].

Thus, the continuous observation of the parent and daughter ions excludes any possible time-dependent alteration of the detection efficiency [28]. The ion-optical mode used for running the ESR guarantees that the daughter ions remain in the apparatus, therefore a uniform detection efficiency for the  $4\pi$  solid angle is provided.

Since the times related to the appearance of the daughter ion trace in the Schottky spectrum could be determined more precisely than the decay times, only those were taken into consideration for the further analysis. The decay times from each of the three experiments mentioned above were combined together yielding time distributions of the electron capture events for each of them. A time modulated decay probability of the orbital electron capture has been observed for H-like  $^{140}\text{Pr}^{58+}$ ,  $^{142}\text{Pm}^{60+}$  [28] and as a preliminary result for  $^{122}\text{I}^{52+}$  ions. As an example the results of the  $^{140}\text{Pm}$  measurement are presented in Fig. 3. A fit procedure involving a pure exponential decay function (continuous line in Fig. 3) does not reproduce the measured data, hence a superimposed periodic time modulation has been included in the model used for the data estimation:

$$\frac{dN_{\text{EC}}(t)}{dt} = N_{\text{EC}}(0)e^{-\lambda t} \lambda_{\text{EC}}(t), \quad (6)$$

where a time dependent decay probability can be expressed as

$$\lambda_{\text{EC}}(t) = \lambda_{\text{EC}}(1 + a \cos(\omega t + \phi)), \quad (7)$$

and  $a$  is the modulation amplitude,  $\omega$  the angular frequency and  $\phi$  is the phase of the modulation. A modulation period of  $T = 7.06(8)$  s for  $^{140}\text{Pr}$ ,  $T = 7.10(22)$  s for  $^{142}\text{Pm}$  and preliminarily  $T \simeq 6.0$  s for  $^{122}\text{I}$  has been



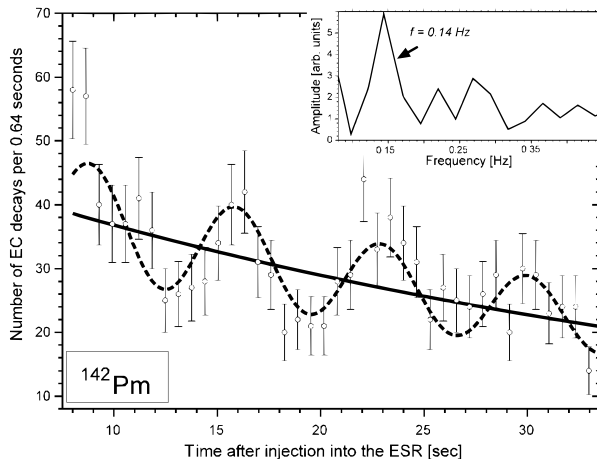


Fig. 3. Decay rate of  $^{142}\text{Pm}$ . The solid line shows a pure exponential fit, the dashed line includes a superimposed modulation. The inset shows the FFT spectrum obtained from these data [28].

observed. A summary on the fit results is given in Table II. The almost constant value of the  $T/M$  ratio included in the last column of Table II could indicate that the modulation period  $T$  might scale with the mass  $M$  of the decaying system [28, 29]. This statement is based on the preliminary value of the modulation period  $T$  for  $^{122}\text{I}$ , though.

TABLE II

Summary of the fit results of the data collected for the  $^{140}\text{Pr}$ ,  $^{142}\text{Pm}$  and the preliminary results for  $^{122}\text{I}$ . All values for  $\omega$  and  $T$  are given in the laboratory frame. More detailed compilation of the experimental results can be found in Refs. [28, 29].

$M$ [amu]	$\omega$ [ $\text{s}^{-1}$ ]	$T_{\text{lab}}$ [s]	$a$	$T/M$ [s/amu]
122	$\sim 1.04^*$	$\sim 6.0^*$	$\sim 0.2^*$	$\sim 0.05^*$
140	0.890(10)	7.06(8)	0.18(3)	0.0504(5)
142	0.885(27)	7.10(22)	0.23(4)	0.0500(10)

\*Preliminary results.

An attempt of explaining the origin of these striking results had already been formulated as a hypothesis by one of the authors (F.B.) long before these experiments were performed. If one considers the emitted electron neutrino as a superposition of at least two mass eigenstates [28, 30] an over-

lap of the energies of the massive neutrino mass eigenstate and of the wave functions of the daughter ions is caused by the energy and momentum uncertainties introduced by the time differential detection of the daughter ions in GSI experiments [30]. A recently developed theory suggests the modulation period to be proportional to the mass of the parent ion, thus remaining in agreement with the tentative experimental result [30].

We have to stress that according to the preliminary data for the three-body  $\beta^+$  decay of  $^{142}\text{Pm}$  the modulation is not present in the decay time distribution. This suggests that the effect is solely related to monoenergetic neutrinos and experimental effects and nuclear properties of the initial state can be excluded. A much more detailed discussion of the described phenomenon can be found in Refs. [28, 30].

#### 4. Summary

The technique of Schottky lifetime spectroscopy has been applied to explore the electron capture and bound-state  $\beta^-$  decay processes of ions circulating in the ESR.

The electron-capture decay rate measurements for H-like  $^{140}\text{Pr}$  and  $^{142}\text{Pm}$  show that reduction of the number of shell electrons in the decaying atom can increase the probability of the electron capture transition. The obtained results are explained by taking into account the conservation of the total angular momentum of the nucleus-lepton system and including the hyperfine interaction in the theory of the electron capture decay. As a next step the measurement of the H-like  $^{64}\text{Cu}$  lifetime is scheduled [31]. The negative value of its magnetic momentum assigns the lower hyperfine state to the  $F = 3/2$  total angular momentum. Therefore, the electron capture transition to the  $^{64}\text{Ni}$  ground state ( $I_f = 0$ ,  $F = 1/2$ ) should be strongly hindered.

We report on the direct observation of bound-state  $\beta^-$ -decays of fully-ionized  $^{205}\text{Hg}^{80+}$  and  $^{207}\text{Tl}^{81+}$  atoms. The obtained results are in good overall agreement with the predictions of the theory employing spectra of allowed transition. However, the  $\lambda_{\beta_c}$  decay rate for bare  $^{205}\text{Hg}$  nuclei was found to be smaller comparing to the results of the calculations.

The continuation of this research programme could focus on investigation of the  $\beta_b$ -decay phenomenon in  $^{205}\text{Tl}$  [32] being of great importance for the solar neutrino flux determination [33].

Time dependent Schottky Noise Spectrometry may appear as a new method for studying neutrino properties investigating two body decays in a storage ring where ions are kept in quasi free conditions [28, 34]. A time modulated decay probability of the orbital electron capture has been observed for H-like  $^{140}\text{Pr}^{58+}$  and  $^{142}\text{Pm}^{60+}$  ions. The preliminary analysis indicates a similar behaviour of the decay rate probability for  $^{122}\text{I}^{52+}$ . A possible explanation of this results is given by considering the emitted electron neutrino as

a superposition of at least two mass eigenstates. We should emphasize that this interpretation is broadly disputed [35–37] and needs an urgent experimental confirmation or disproval. Our preliminary results suggests that the modulation period might scale with the mass  $M$  of the decaying nucleus. This finding would remain in agreement with the prediction of a recently developed theoretical model.

## REFERENCES

- [1] F. Bosch, *Phys. Scr.* **T59**, 221 (1995).
- [2] M. Jung *et al.*, *Phys. Rev. Lett.* **69**, 2164 (1992).
- [3] H. Irnich *et al.*, *Phys. Rev. Lett.* **75**, 4182 (1995).
- [4] B. Franzke, H. Geissel, G. Müntenberg, *Mass. Spectrom. Rev.* **27**, 428 (2008).
- [5] H. Geissel *et al.*, *Nucl. Instrum. Methods Phys. Res.* **B70**, 286 (1992).
- [6] B. Franzke, *Nucl. Instrum. Methods Phys. Res.* **B24/25**, 18 (1987).
- [7] T. Radon *et al.*, *Phys. Rev. Lett.* **78**, 4701 (1997).
- [8] S. van der Meer, *Rev. Mod. Phys.* **57**, 689 (1985) and references therein.
- [9] F. Nolden *et al.*, *Nucl. Instrum. Methods Phys. Res.* **A441**, 219 (2000).
- [10] G.I. Budker, *At. Energ.* **22**, 346 (1967) [*Sov. J. At. Energy* **22**, 438 (1967)].
- [11] M. Steck, P. Beller, K. Beckert, B. Franzke, F. Nolden, *Nucl. Instrum. Methods Phys. Res.* **A532**, 357 (2004).
- [12] B. Schlitt *et al.*, *Hyper. Int.* **99**, 117 (1996).
- [13] T. Radon *et al.*, *Nucl. Phys.* **A677**, 75 (2000).
- [14] F. Bosch *et al.*, *Int. J. Mass. Spectr.* **251**, 212 (2006).
- [15] Yu.A. Litvinov *et al.*, *Phys. Rev. Lett.* **99**, 262501 (2007).
- [16] H. Geissel *et al.*, *Eur. Phys. J. Special Topics* **150**, 109 (2007).
- [17] W. Bambynek *et al.*, *Rev. Mod. Phys.* **49**, 77 (1977).
- [18] I.N. Borzov, E.E. Saperstein, S.V. Tolokonnikov, *Phys. At. Nucl.* **71**, 469 (2008).
- [19] Z. Patyk *et al.*, *Phys. Rev.* **C77**, 014306 (2008).
- [20] A.N. Ivanov, M. Faber, R. Reda, P. Kienle, *Phys. Rev.* **C78**, 025503 (2008).
- [21] N. Winckler *et al.*, *Phys. Lett.* **B679**, 36 (2009).
- [22] F. Bosch *et al.*, *Phys. Rev. Lett.* **77**, 5190 (1996).
- [23] K. Takahashi, K. Yokoi, *Nucl. Phys.* **A404**, 578 (1983).
- [24] M. Faber *et al.*, *Phys. Rev.* **C78**, 061603(R) (2008).
- [25] T. Ohtsubo *et al.*, *Phys. Rev. Lett.* **95**, 052501 (2005).
- [26] F. Attallah *et al.*, *Nucl. Phys.* **A701**, 561c (2002).
- [27] Yu.A. Litvinov *et al.*, *Nucl. Phys.* **A756**, 3 (2005).

- [28] Yu.A. Litvinov *et al.*, *Phys. Lett.* **B664**, 162 (2008).
- [29] N. Winckler *et al.*, GSI Scientific Report 2008, 2009-01, 160 (2009).
- [30] A.N. Ivanov, P. Kienle, *Phys. Rev. Lett.* **103**, 062502 (2009).
- [31] Yu.A. Litvinov *et al.*, proposal E078 for an experiment at GSI (2007).
- [32] F. Bosch *et al.*, proposal for an experiment at GSI (2003).
- [33] M. Freedman, *Nucl. Instrum. Methods Phys. Res.* **A271**, 267 (1998).
- [34] P. Kienle, *Nucl. Phys.* **A827**, 510c (2009).
- [35] C. Giunti, *Phys. Lett.* **B665**, 92 (2008).
- [36] A. Cohen, S. Glashow, Z. Ligati, *Phys. Lett.* **B678**, 191 (2009).
- [37] C. Giunti, *Nucl. Phys.* **B188**, 43 (2009).